Supplementary Table 1. Data collection and refinement statistics (molecular replacement).

Data set statistics	HLA A*0201-ALWGPDPAAA	PPI TCR	PPI TCR/A2-ALWGPDPAAA	PPI TCR/A2-ALWGPDPAAA
Space Group	$P2_1$	$C2_1$	P1	$P2_1$
Unit Cell parameters (Å,°)	a=53.1, b=81.15, c=56.55, β=112.87	a=192, b=43.26, c=124.71, β =101.25	a=41.48, b=98.44, c=121.30, α=97.27, β=98.15, γ=93.37	a=93.68, b=84.59, c=126.28, β=90.03
Radiation Source	DIAMOND I03	DIAMOND I24	DIAMOND I03	DIAMOND I03
Wavelength (Å)	0.9763	0.9778	0.9763	0.9763
Resolution (Å)	45.59 - 1.67 (1.714 - 1.670)	30.58 - 2.57 (2.64 - 2.57)	100.0 - 2.60 (2.70 - 2.60)	63.14 - 2.71 (2.78 - 2.71)
Unique reflections	50142 (3594)	32415 (2358)	55948 (5876)	53460 (3894)
Completeness (%)	98.1 (94.8)	99.6 (99.8)	96.9 (96.5)	99.4 (99.4)
Multiplicity	4.0 (4.0)	3.7 (3.6)	2.1 (2.2)	4.1 (4.2)
I/Sigma(I)	16.2 (2.2)	9.3 (1.8)	11.76 (2.48)	11.1 (2.1)
Rmerge (%)	5.0 (57.0)	8.2 (78.2)	5.4 (36.1)	8.5 (70.6)
Refinement statistics (highest resolution shell in parenthesis)				
MR Input Model	2P5E (A,B,C)	P1 model	2P5E & 3HG1	P1 model
No reflections used	47597	30770	51877	50745
No reflections in Rfree set	2545	1644	2634	3713
Rcryst (no cutoff) (%)	19.5	22.9	19.5	20.1
Rfree (%)	24.4	29.1	27.4	26.9
RMSD from ideal geometry (target values in parenthesis)				
Bond lengths (Å)	0.022 (0.021)	0.016 (0.022)	0.003	0.014 (0.021)
Bond Angles (°)	2.182 (1.922)	0.905 (1.954)	0.671	1.244 (1.935)
Mean B value ($Å^2$)	18.8	50.19	n/m	52.5
Wilson B-factor ($Å^2$)	19.8	67.4	38.09	67.8
Outliers Ramachandran plot (%)	0	1.8	1.2	0.97
Overall ESU based on Maximum Likelihood (Å)	0.084	0.319	0.39	0.32

One crystal was used for data collection.
n/m: not measured
*Values in parentheses are for highest-resolution shell.

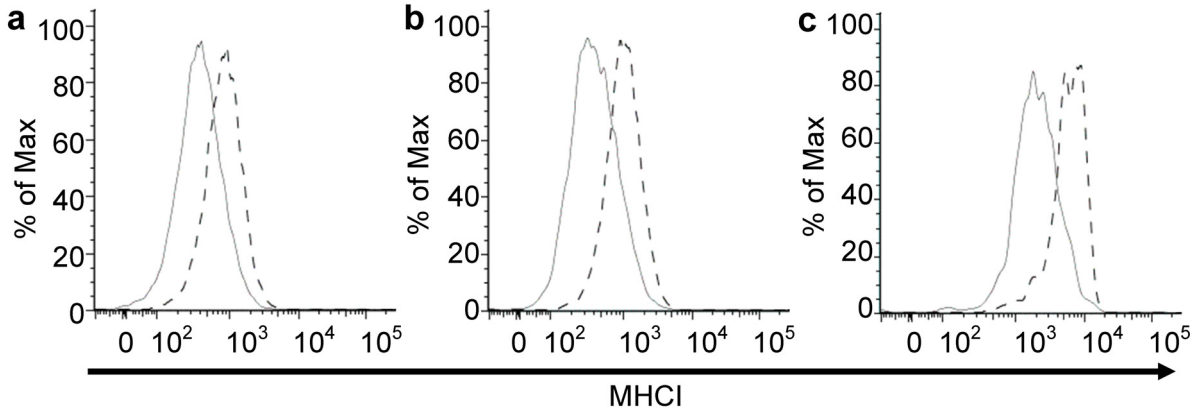

Supplementary Figure 1: Flow cytometric analysis of MHCI up-regulation after treatment of islet cells purified from 3 HLA-A*0201+ donors and treated with IL-1β, TNF and IFN-γ. **(a-c;** organs donors 1-3, respectively) Staining with the PE-conjugated pan-class I mAb W6/32 is shown for islet cells before (solid line) and after (dashed line) MHCI upregulation.

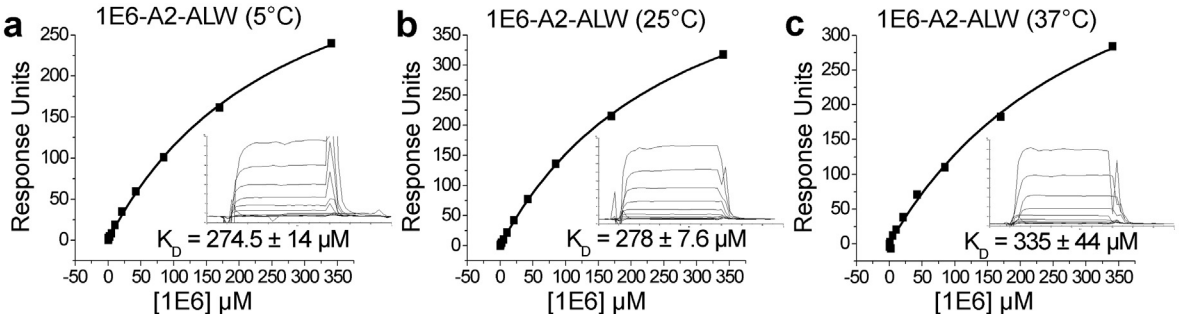

Supplementary Figure 2. Binding affinity of the 1E6-A2-ALW interaction at 5, 25 and 37°C. Ten serial dilutions of the 1E6 TCR were measured in triplicate at each temperature; representative data from these experiments are plotted. **(a-c).** The equilibrium binding constant (K_D) values were calculated using a nonlinear curve fit ($y= (P_1x)/P_2 + x)$); mean plus SD values are shown. In order to calculate each response, the 1E6 TCR was also injected over a control sample (HLA-A*0201 in complex with ELAGIGILTV peptide) that was deducted from the experimental data (shown in the inset).

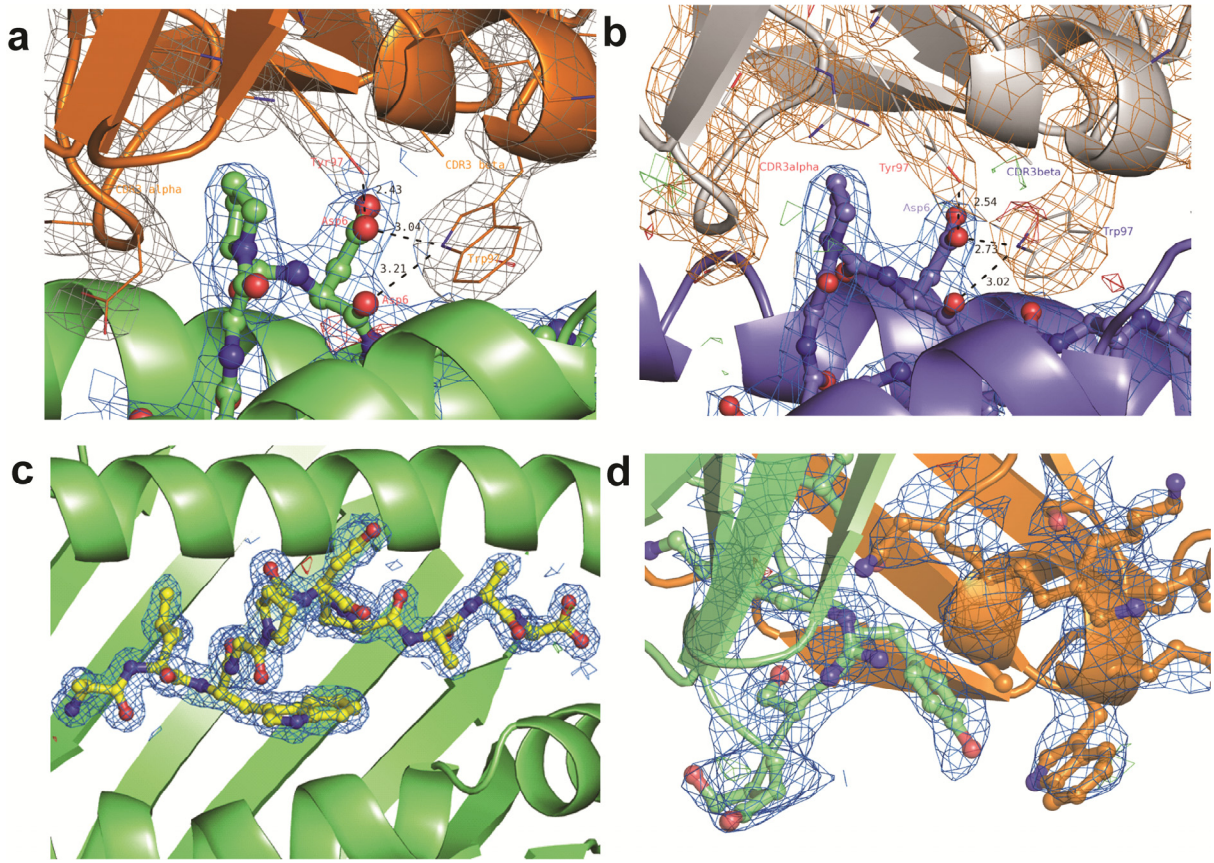

Supplementary Figure 3: 2Fo-Fc electron density maps for the 1E6-A2-ALW complex, uncomplexed A2-ALW and uncomplexed 1E6 TCR models. All maps shown are within 2Å from the atoms to which they relate. **(a)** 1E6-A2-ALW at the interface between the TCR (density shown in grey) and the GPD peptide (density shown in blue) motif in copy 1 contoured at 1.5σ. **(b)** 1E6-A2-ALW at the interface between the TCR (density shown in orange) and the GPD peptide (density shown in blue) motif in copy 2 contoured at 1.5σ. **(c)** Uncomplexed A2-ALW looking down on top of ALW (density shown in blue) contoured at 1σ. **(d)** Electron density around the CDR3α and β loops of the uncomplexed 1E6 TCR (density shown in blue) contoured at 1σ.

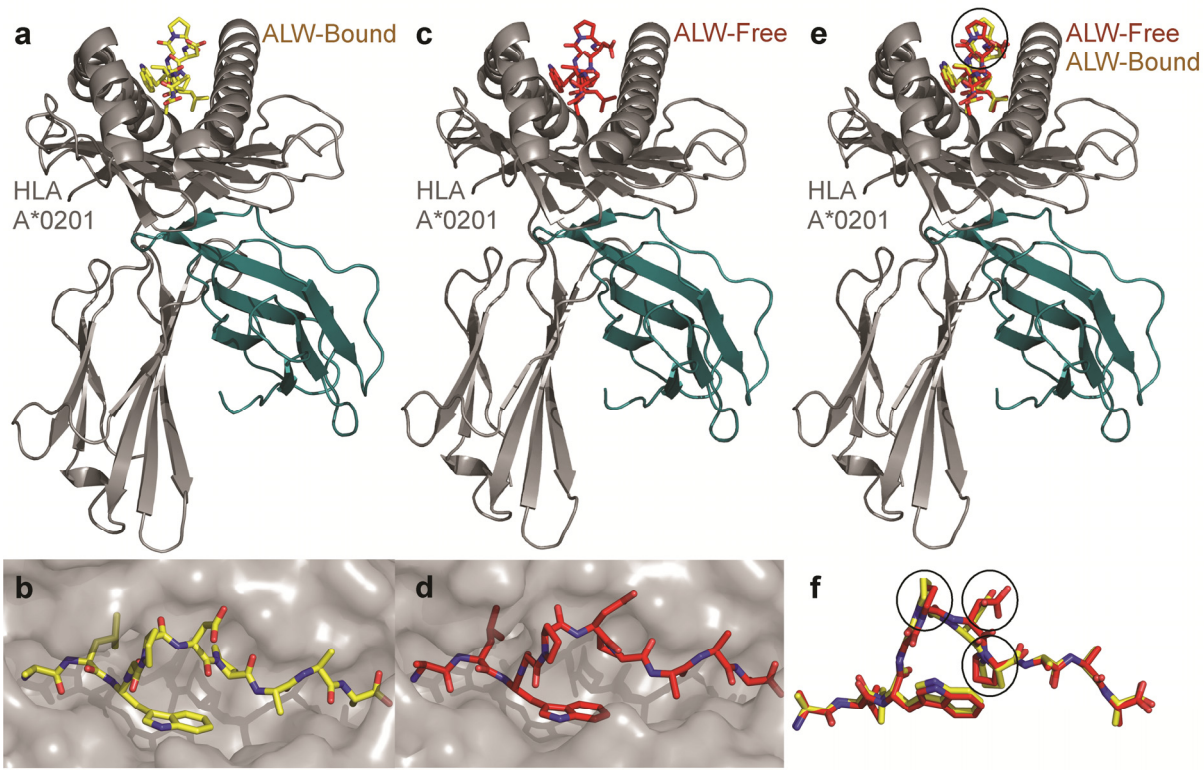

Supplementary Figure 4: Conformation of A2-ALW in complex with the 1E6 TCR *versus* A2-ALW uncomplexed. **(a)** Conformation of A2-ALW in complex with the 1E6 TCR (1E6 TCR omitted). **(b)** Orientation looking from above at the conformation of the bound ALW peptide (yellow sticks) with the MHC shown as surface (grey)**. (c)** Conformation of free A2-ALW. **(d)** Orientation looking from above at the conformation of the free ALW peptide (red sticks) with the MHC shown as surface (grey). **(e)** Superposition of the free (red) and complexed (yellow) ALW peptides in the context of HLA A*0201. **(f)** Orientation looking from above at the conformation of the free (red) and complexed (yellow) ALW peptides superposed. Some small conformational changes could be observed at Pro5, Asp6 and Pro7 (circled).

Structure of uncomplexed A2-ALW:

Previous investigations have shown that both the peptide[1] and the MHC[2] can undergo conformational changes during TCR binding. The structure of A2-ALW was solved at 1.67Å and refinement gave a model with 100% of residues in the preferred and allowed regions of the Ramachandran plot and geometry consistent with the data resolution (**Supplementary Table 1, Supplementary Fig. 2c**). The crystallographic R/Rfree factors were 19.5% and 24.4% respectively, and fell in the expected ratio range[3]. Superposition of the 1E6 TCR complexed A2-ALW molecule (**Supplementary Fig. 3a and Fig. 3b**) and the free A2-ALW (**Supplementary Fig. 3c and Fig. 3d**) models showed that the overall conformations were virtually identical. Some small movements could be observed in the solvent exposed side chains of Pro5, Asp6 and Pro7 (**Supplementary Fig. 3e and Fig. 3f**), but these relatively minor changes were unlikely to govern TCR binding.

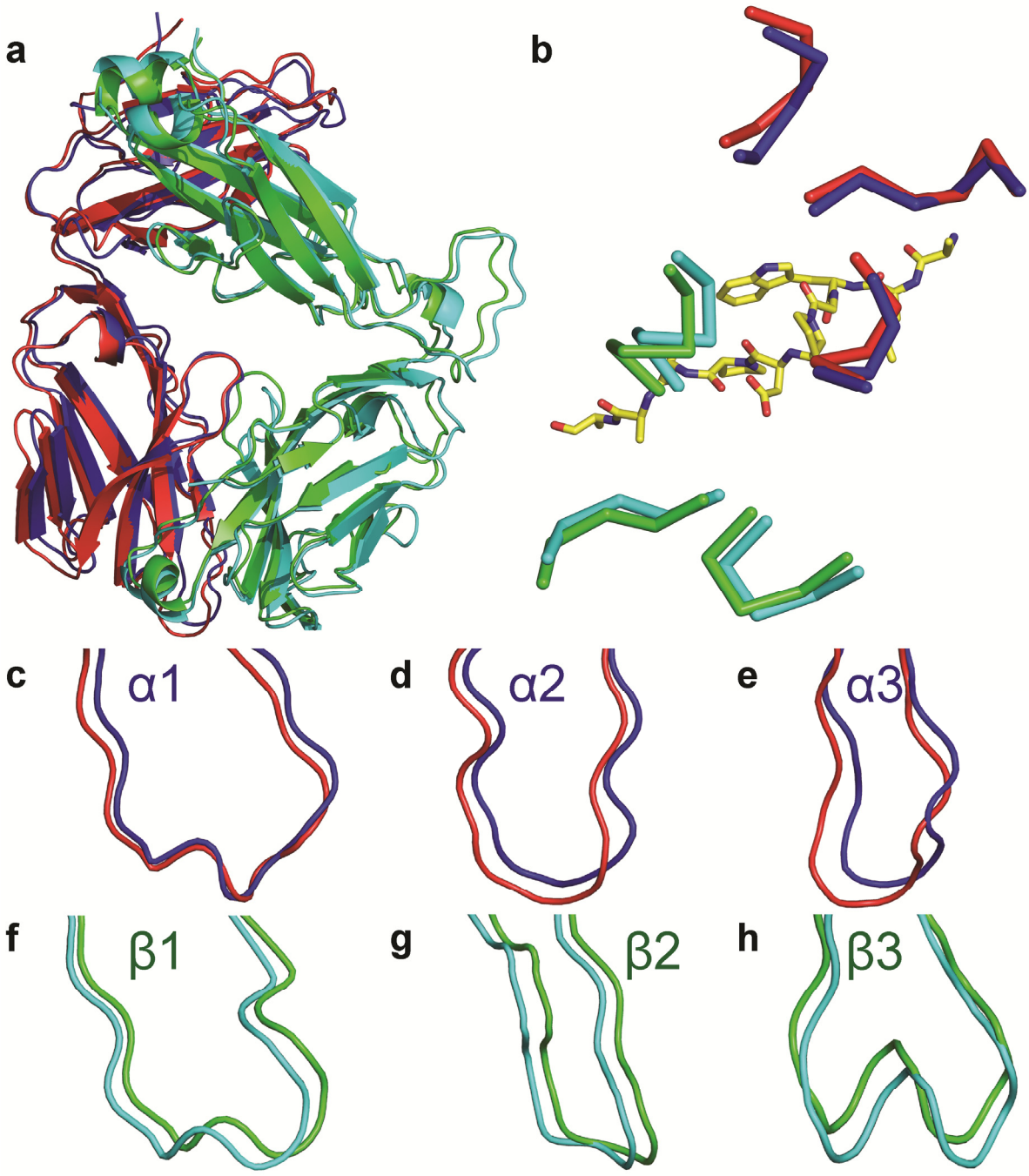

Supplementary Figure 5: Comparison of the conformation of the 1E6 TCR CDR1, CDR2 and CDR3 loops in the 1E6-A2-ALW complex *versus* 1E6 TCR uncomplexed. **(a)** Superposition of the free (red and cyan cartoon) and complexed (blue and green cartoon) 1E6 TCR. **(b)** Superposition of the free (red and cyan lines) and complexed (blue and green lines) 1E6 TCR looking down on the peptide (yellow sticks). **(c)** Superposition of the free (red cartoon) and complexed (blue cartoon) 1E6 TCR CDR1α loop. **(d)** Superposition of the free (red cartoon) and complexed (blue cartoon) 1E6 TCR CDR2α loop. **(e)** Superposition of the free (red cartoon) and complexed (blue cartoon) 1E6 TCR CDR3α loop. **(f)** Superposition of the free (cyan cartoon) and complexed (green cartoon) 1E6 TCR CDR1β loop. **(g)** Superposition of the free (cyan cartoon) and complexed (green cartoon) 1E6 TCR CDR2β loop. **(h)** Superposition of the free (cyan cartoon) and complexed (green cartoon) 1E6 TCR CDR3β loop.

Structure of the uncomplexed 1E6 TCR:

The flexible TCR CDR-loops have been shown to undergo numerous, and sometimes large, conformational changes upon pMHC binding[4]. To date, there exist only 5 examples of both free and complexed human TCRs[4, 5] providing a rare insight into the mechanism that governs TCR antigen recognition and cross-reactivity. We solved the structure of the 1E6 TCR at 2.57Å (**Supplementary Table 1, Supplementary Fig. 2d**). Refinement resulted in a model with 98.2% of residues in the preferred and allowed regions of the Ramachandran plot and geometry consistent with the data resolution. The crystallographic R/Rfree factors were 22.9% and 29.1%, consistent with the expected ratio range[3]. Superposition of the free and the bound 1E6 TCR showed that the overall conformations were virtually identical (**Supplementary Fig. 4a**). Similarly, the overall positions of the TCR CDR-loops were conserved before and after binding to A2-ALW (**Supplementary Fig. 4b**). Closer inspection of the TCR CDR loops showed that, in accordance with previously published work, the CDR1 and 2 loops exhibited only modest changes in position compared with the CDR3 loops before and after pMHC docking[4]. The CDR1 and CDR2 loops underwent a small rigid body shift of ≤1Å (**Supplementary Fig. 4c, Fig. 4d, Fig. 4f and Fig. 4g**). Additionally, the CDR2 loops exhibited a small degree of hinge bending. Both of the CDR3 loops displayed a larger degree of conformational change including an average hinge movement of ~1.5Å (**Supplementary Fig. 4e and Fig. 4h**). These changes were relatively minor compared to other structural studies (JM22[6, 7] exhibited the largest loop movement of 5.6Å). Overall, the 1E6 TCR requires only a moderate level of CDR loop plasticity in order to dock with A2-ALW.

References:

1. Tynan, F.E. *et al.* A T cell receptor flattens a bulged antigenic peptide presented by a major histocompatibility complex class I molecule. *Nat Immunol* **8**, 268-276 (2007).
2. Borbulevych, O.Y. *et al.* T cell receptor cross-reactivity directed by antigen-dependent tuning of peptide-MHC molecular flexibility. *Immunity* **31**, 885-896 (2009).
3. Tickle, I.J., Laskowski, R.A. & Moss, D.S. Rfree and the rfree ratio. II. Calculation Of the expected values and variances of cross-validation statistics in macromolecular least-squares refinement. *Acta Crystallogr D Biol Crystallogr* **56**, 442-450 (2000).
4. Armstrong, K.M., Piepenbrink, K.H. & Baker, B.M. Conformational changes and flexibility in T-cell receptor recognition of peptide-MHC complexes. *Biochem J* **415**, 183-196 (2008).
5. Archbold, J.K. *et al.* Natural micropolymorphism in human leukocyte antigens provides a basis for genetic control of antigen recognition. *J Exp Med* **206**, 209-219 (2009).
6. Kjer-Nielsen, L. *et al.* The 1.5 A crystal structure of a highly selected antiviral T cell receptor provides evidence for a structural basis of immunodominance. *Structure (Camb)* **10**, 1521-1532 (2002).
7. Stewart-Jones, G.B., McMichael, A.J., Bell, J.I., Stuart, D.I. & Jones, E.Y. A structural basis for immunodominant human T cell receptor recognition. *Nat Immunol* **4**, 657-663 (2003).